Adsorption (2013) 19:1007–1018
DOI 10.1007/s10450-013-9511-x

Nonlinear direct inverse method: a shortcut method for simultaneous calibration and isotherm determination

Bijan Medi · Monzure-Khoda Kazi · Mohammad Amanullah

Received: 15 November 2012 / Accepted: 7 February 2013 / Published online: 21 February 2013

Abstract This work addresses a way to combine isotherm determination and nonlinear calibration. In this method, like the classical inverse method, experimental elution profiles are compared with the results of a detailed model that accounts for nonlinearity in equilibrium, axial dispersion, and mass transfer kinetics. However, unlike the classical inverse method, the calibration of detector is carried out simultaneously with isotherm determination thereby reducing cost and saving time. In this study no limitation is imposed on the linearity of the detector signal or on the overlapping of elution profiles for the separation of enantiomers. The method has been experimentally validated for the separation of a mixture of guaifenesin enantiomers over a wide range of concentration.

Keywords Enantioseparation · Inverse method · Preparative chromatography · Guaifenesin · Genetic algorithm

List of symbols

a	Slope of absolute calibration equation (g/L/mAU)
b	Intercept of absolute calibration equation (g/L)
c	Nonlinear parameter of absolute calibration equation (1/mAU)
$c(t)$	Fluid phase concentration of solute (g/L)
c_T^F	Total feed concentration (g/L)
D	Column diameter (cm)
D_{ax}	Axial dispersion coefficient (m^2/s)
d_p	Particles diameter (μm)
E	Estimation error (–)
H_i	Henry constant of species i (–)
K_i	Equilibrium constant in Langmuir isotherm of species i (L/g)
k_i	Overall mass transfer coefficient (1/s)
L	Column length (cm)
N_{cy}	Number of experiment cycles (–)
$N_{t,j}$	Number of discretized data points collected over time for the jth experiment (–)
n	Solid phase concentration of solute (g/L)
n^*	Equilibrium solid phase concentration of solute (g/L)
S	Peak area (mAU s)
Q	Volumetric flow rate (mL/min)
$q_{s,i}$	Saturation capacity of species i (g/L)
t	Time (s)
t_e	End time of experimental run (s)
t_p	Feed pulse width (s)
v	Interstitial velocity (cm/s)
V_d	Extra column dead volume (μL)
V_{inj}	Injection volume (μL)
y	Absorbance (mAU)
z	Axial coordinate (cm)

Greek letters

α	Slope of analytical calibration line (mAU s L/g)
β	Intercept of analytical calibration line (mAU s)
ε	Overall void fraction of column (–)
λ	Penalty factor (-)

Subscripts and superscripts

A	More retained component
ax	Axial
B	Less retained component

B. Medi · M. K. Kazi
School of Chemical and Biomedical Engineering, Nanyang Technological University, 62 Nanyang Drive, Singapore 637459, Singapore

M. Amanullah (✉)
Department of Chemical Engineering, College of Engineering, Qatar University, P.O. Box 2713, Doha, Qatar
e-mail: Aman@qu.edu.qa

exp Experimental
F Feed
i Component index
inj Injection
ns Non-selective
sim Simulation

1 Introduction

Adsorption isotherms describe the equilibrium with which the solute molecules are divided between fluid phase and adsorbent. In chromatographic separation technology, adsorption isotherm plays a significant role in process design and optimization. Although several experimental methods with varying levels of accuracy are available for isotherm determination (Ruthven 1984; Guiochon et al. 2006; Seidel-Morgenstern 2004), it is still a tedious and laborious task. Therefore, determination of adsorption isotherm parameters accurately is always challenging for designers and practitioners.

In preparative chromatography, it is not straightforward to estimate the isotherm parameters through correlations considering the system complexity (Guiochon et al. 2006), and therefore experimental efforts are always necessary, which can be carried out in various ways. In this regard, there is a compromise necessary between the accuracy and cost (time, labor, and materials) of experiments (Rajendran and Chen 2009).

Static methods such as gravimetry (Thompson and Fuller 1987), volumetry, and infrared absorption (Soussen-Jacob et al. 1989) or dynamic methods such as frontal analysis (FA) (Lisec et al. 2001), perturbation method (PM) (Blumel et al. 1999), elution by characteristic points (ECP), and inverse method (IM) (Felinger et al. 2003) have been used for isotherm determination. Static methods are typically slow and mostly used for gas adsorption (Rajendran and Chen 2009), whereas dynamic methods which involve the flow of a fluid through a column packed with stationary phase, are well suited for liquid chromatography.

The conventional methods such as FA can estimate both single and multi-component isotherms, but they require a significant number of experiments and amount of materials. The inverse method alleviates these requirements to some extent. Hence, it has been extensively applied in various fields (Juza et al. 2000; Guiochon 2002; Wenda and Rajendran 2009; Cornel et al. 2010). However, IM and many other dynamic methods require calibration of detector signals to convert into concentration values (Rajendran and Chen 2009). This is generally a time-consuming step and is an important source of error in isotherm determination tasks. Moreover, in the case of achiral compounds, where the elution profiles overlap, the problem becomes aggravated (Cornel et al. 2010). Considering these factors, Cornel et al. (2010) have proposed a modified version of inverse method called direct inverse method (DIM) to circumvent calibration. This method directly utilizes the detector signal without any need for a separate calibration. It was shown that this approach was equally applicable in the case of strongly overlapping profiles. Nevertheless, the main limitation of DIM has been the requirement of the linearity of the calibration equation emanating from the solution approach (Cornel and Mazzotti 2008). In chromatographic processes however, nonlinearity of the detector signals due to overloaded solute concentration is very common. Moreover, this method necessitates use of a diode-array detector and collection of large amount of data produced during every experimental run. Therefore, an extension of the DIM to encompass nonlinear calibration is necessary and useful for a wider range of separation and higher degree of accuracy.

In this work, we propose a nonlinear direct inverse method (NDIM) whose application is not limited to linear calibration equations. This method is in fact different from what developed by Cornel et al. (2010) as the calibration procedure is carried out at the same time with isotherm determination (in contrast to the classical inverse method, (Guiochon et al. 2006)), by comparing simulated and experimental concentration profiles in order to obtain the best-fit parameters. The detector calibration parameters, isotherm parameters, and transport parameters (mass transfer and axial dispersion coefficients) are incorporated as the decision variables of an optimization problem.

Due to a large number of decision variables and nonlinearity of the detector response and adsorption isotherm that describes the separation behavior, this optimization problem is of a challenging nature. Therefore, genetic algorithm (GA) (Goldberg 1989) is used here to search for the optimum values in combination with sequential quadratic programming (SQP), which is a classical but efficient gradient-based optimization technique (Lawrence and Tits 2001), to pinpoint the final solution.

2 Problem formulation

2.1 Modeling

Various models with different levels of details are available in the literature for simulating chromatographic systems (Guiochon et al. 2006). A one-dimensional model, which considers convection and axial dispersion in the fluid phase, is employed here. In addition, linear driving force model is used for approximating mass transfer kinetics,

which is a good approximation at least for efficient chromatographic columns in the absence of other non-idealities such as non-homogeneous packing. The material balance and mass transfer kinetics are expressed by the following equations, respectively

$$\frac{\partial c_i}{\partial t} + \frac{1-\varepsilon}{\varepsilon}\frac{\partial n_i}{\partial t} + v\frac{\partial c_i}{\partial z} = D_{ax,i}\frac{\partial^2 c_i}{\partial z^2} \tag{1}$$

$$\frac{\partial n_i}{\partial t} = k_i\left(n_i^* - n_i\right) \tag{2}$$

here t and z are the time and space coordinates, respectively. ε is the overall void fraction of column and v is the interstitial velocity. n_i^* is the solid phase concentration in equilibrium with fluid phase concentration c_i. $D_{ax,i}$ is axial dispersion coefficient and k_i is overall mass transfer coefficient of species i.

The initial conditions for these equations are as follows:

$$c_i(0,z) = 0, \quad n_i(0,z) = 0 \tag{3}$$

For Eq. 1, the Danckwerts' boundary conditions apply at inlet and outlet:

$$D_{ax,i}\frac{\partial c_i(t,0^+)}{\partial z} = v(c_i(t,0^+) - c_i^{in}(t)), \quad \frac{\partial c_i(t,L)}{\partial z} = 0 \tag{4}$$

where $c_i^{in}(t)$ is defined as:

$$c_i^{in}(t) = \begin{cases} c_i^F & \text{if } 0 \le t \le t_p \\ 0 & \text{else} \end{cases} \tag{5}$$

This definition implies that feed is ideally injected as a rectangular pulse with width t_p. In reality however, this is a simplistic assumption because axial dispersion in injection mechanism may distort the injection pulse in an asymmetric way (Asnin et al. 2005), causing tailing in extreme cases even when no column is installed in the flow path. These effects will be discussed in the results section.

In the classical inverse method (referred to as CIM here), often mass transfer and axial dispersion effects are lumped together (Wenda and Rajendran 2009). However, Dunnebier and Klatt (2000) argue that this is theoretically correct only in the case of linear isotherms, and it is a good approximation for Langmuir isotherm as originally investigated by Golshanshirazi and Guiochon (1992). As we are using a bi-Langmuir isotherm, it is prudent to separate these effects in the modeling and parameter estimation.

It must be noted that mass transfer resistance has two separate effects; on one hand, it affects band broadening, and on the other hand, it affects retention time and thus changes apparent Henry constants. Therefore, when a significant level of mass transfer resistance prevails (i.e., k_i is small), the Henry constants measured via analytical injections must not be used in a model equation that explicitly includes mass transfer limitations. This may explain the difference occasionally observed between the Henry constants measured by direct retention time measurement and those by the classical inverse method (Wenda and Rajendran 2009). The effects of change in mass transfer coefficients are investigated via simulation in Sect. 5.

2.2 Isotherms

A competitive Langmuir isotherm accounting for competition and a finite number of sites is given as:

$$n_i = \frac{q_{s,i}K_i c_i}{1 + \sum_{i=1}^{N_c} p_i K_i c_i} \tag{6}$$

where, $q_{s,i}$ is the saturation capacity of the adsorbent and K_i is the equilibrium constant of adsorption for component i. p_i is the parameter that shows the type of competition, and can only take 1 and -1 values. For a binary system, four types of Langmuir isotherms can be obtained (Mazzotti 2006). The classical competitive Langmuir isotherm is obtained for $p_1 = 1$ and $p_2 = 1$. For simplicity, we drop these parameters from our formulations.

In practical applications, it is more convenient to write the above equation in terms of Henry constants:

$$n_i = \frac{H_i c_i}{1 + \sum_{i=1}^{N_c} K_i c_i} \tag{7}$$

where

$$H_i = q_{s,i}K_i \tag{8}$$

for some separations, especially in chiral chromatography equilibrium is described by a bi-Langmuir isotherm, which accounts for both selective and non-selective adsorption (Amanullah and Mazzotti 2006):

$$n_i = \frac{H_i c_i}{1 + \sum_{i=1}^{N_c} K_i c_i} + \frac{H_{ns} c_i}{1 + \sum_{i=1}^{N_c} K_{ns} c_i} \tag{9}$$

H_{ns} and K_{ns} are non-selective parameters, but carry the same definition as given for selective parameters above. Furthermore, we must point out here that we do not assume equal saturation capacities for the isotherms employed here.

2.3 Calibration equations

While satisfying material balance, a calibration equation takes into account absorbance intensity and signal value at baseline. Therefore, for linear operating range:

$$c(t) = ay(t) + b \tag{10}$$

where, $y(t)$ is the detector signal in an appropriate unit (e.g., mAU) collected as a function of time. The parameter a is a

constant which is inversely proportional to absorbance intensity, and the term $-b/a$ is the signal value at baseline. This direct formulation of concentration versus detector signal is sometimes called absolute calibration (Asnin et al. 2005).

Since nonlinearity of the detector signal is expected, we propose the following rational and exponential equations:

$$c(t) = \frac{ay(t) + b}{(cy(t) + 1)^2} \tag{11}$$

$$c(t) = ay(t)e^{-cy(t)} + b \tag{12}$$

It may be noted that both of the nonlinear equations reduce to the linear equation at low $y(t)$ values. Therefore, the term $-b/a$ is the signal value at baseline for these equations as well. This information will be used to enhance the convergence of the parameter estimation technique as will be described in Sect. 3.1

The two nonlinear equations given above contain three degrees of freedom each. Using higher degrees of freedom is not recommended because of the risk of overfitting when the experimental data is scarce.

3 Parameter estimation

3.1 Calibration

In analytical chromatography, it is customary to calibrate the detector by relating the peak area S to the amount injected, which is called analytical calibration (Asnin and Guiochon 2005) (typically at constant injection volume). In fact the same procedure can be employed for absolute calibration as long as we are in the linear range of absorbance. Under such condition:

$$S = \alpha c_T^F + \beta \tag{13}$$

Since we focus on enatiomers which have identical absorbance characteristics in pure form or as a mixture, total feed concentration c_T^F is used. Assuming that the peak or peaks are completely eluted, we can use material balance to relate Eqs. 13 and 10. Therefore, from material balance we have:

$$Q\int_0^{t_e} c(t)dt = V_{inj}c_T^F \tag{14}$$

where Q and V_{inj} are mobile phase flow rate and sample injection volume, respectively. t_e is the end time of experimental run. We can then replace concentration from Eq. 10 and rearrange this equation:

$$a\int_0^{t_e} y(t)dt + bt_e = \frac{V_{inj}c_T^F}{Q} \tag{15}$$

or

$$aS + bt_e = \frac{V_{inj}c_T^F}{Q} \tag{16}$$

Without further experimental efforts, the parameters a and b can be obtained directly as functions of α and β via comparing Eq. 16 with Eq. 10

$$a = \frac{V_{inj}}{\alpha Q} \tag{17}$$

and

$$b = -\frac{\beta V_{inj}}{\alpha Q t_e} \tag{18}$$

Therefore, as long as we are in the linear range, an analytical calibration yields absolute calibration provided that some extra information about the experimental conditions, namely flow rate, injection volume, and run time are accurately available.

On the other hand, this approach cannot be extended to nonlinear calibration (Asnin et al. 2005; Asnin and Guiochon 2005). In fact the experimental procedure is the same for nonlinear calibration, but it is the solution method that must be revised. One of the effective and economical solutions is again based on using material balance (Asnin and Guiochon 2005; Wenda and Rajendran 2009). In this approach, a predefined form for the calibration equation is assumed, and then the material balance equation is numerically solved as an error minimization problem to obtain the best-fit parameters. In this work, we have defined a slightly modified objective function to improve the accuracy and facilitate convergence:

$$E_C = \sum_{j=1}^{N_{cy}} \frac{\left|Q_j\int_0^{t_e} c_{exp,j}(t)dt - V_{inj,j}c_{T,j}^F\right|}{N_{cy}V_{inj,j}c_{T,j}^F} + \lambda_C \sum_{j=1}^{N_{cy}} \left|\frac{b + a\bar{y}_{j,0}}{N_{cy}\bar{y}_{j,0}}\right| \tag{19}$$

where N_{cy} is the number of experiment cycles. $c_{exp}(t)$ is calculated from any of the equations given earlier (Eqs. 10, 11, 12). $\bar{y}_{j,0}$ is the average baseline signal value for the jth experiment. The role of the second summation in this equation is to enforce zero concentration at baselines for all experiments. As a result, this equation has only three unknowns, namely a, b, and c, which must be obtained implicitly via a numerical optimization procedure.

It must be emphasized that in any of the equations involving integration over time, the integration limits can be reduced to any area around peak or peaks in order to reduce the effects of noise and baseline drift. This approach requires application of peak detection techniques, which is beyond the scope of this work and besides, in our experiments, the improvement was minor. Therefore, the integration range was selected as the entire time interval.

3.2 Isotherm determination

In the classical inverse method, after identifying a proper calibration equation and converting the detector signal to experimental concentration profile, it must be compared with the simulated concentration profile obtained through solving the set of Eqs. 1 and 2 as follows:

$$min\ E_{I1} = \sum_{j=1}^{N_{cy}} \sum_{k=1}^{N_{t,j}} \frac{\left|c_{exp,j}(k) - c_{sim,j}(k)\right|}{N_{cy} N_{t,j} c_{T,j}^{F}} \tag{20}$$

where $N_{t,j}$ is the number of discretized data points collected over time for the jth experiment.

In our approach which is referred to as NDIM throughout this paper, isotherm determination is an extension to the calibration procedure. We just need to combine Eqs. 19 and 20 with proper weight factors to formulate the single objective function of the optimization problem:

$$min\ E_{I2} = E_{I1} + \lambda_{I1} \sum_{j=1}^{N_{cy}} \frac{\left|Q_j \int_0^{t_e} c_{exp,j}(t)dt - V_{inj,j} c_{T,j}^{F}\right|}{N_{cy} V_{inj,j} c_{T,j}^{F}} + \lambda_{I2} \sum_{j=1}^{N_{cy}} \left|\frac{b + a\bar{y}_{j,0}}{N_{cy}\bar{y}_{j,0}}\right| \tag{21}$$

Any integration in the equations above must be carried out numerically. The time delay caused by the dead volume of the experimental setup must be accounted for prior to parameter estimation.

In summary, the decision variables for this optimization problem are isotherm, calibration, and transport parameters. In order to facilitate the convergence, we have carefully constrained the multi-dimensional search space with lower and upper bounds on decision variables. Negative values are not allowed for K_i due to the shape of the experimental concentration profile. The range of decision variables are given in Table 1.

3.3 Optimization algorithms and numerical solution techniques

Literature related to inverse method clearly indicates that solving this problem is of challenging nature. Large number of decision variables and extreme nonlinearities need proper care in this problem. Investigating the calibration problem alone reveals that there are many local minima present in the solution space, adding an extra level of complexity to the overall problem. This is illustrated in Fig. 1 where the objective function E_C is plotted versus a and c around an optimal point. Therefore, a global search approach is more appropriate for this kind of problem. Here we employ GA in single-objective formulation for global search (Amanullah and Mazzotti 2006; Kazi et al. 2012; Goldberg 1989). In every iteration (generation), an entire population is evaluated in a parallel fashion. Although this was a drawback of evolutionary algorithms in the past, thanks to the now-available parallel computing capabilities of commercial computers, it is possible to carry out this task quickly and efficiently.

Table 1 Constraints imposed on the optimization problem

Parameter	Unit	Lower bound	Upper bound
H_A	–	0.1	4.5
K_A	L/g	0	0.05
H_B	–	0.01	2.0
K_B	L/g	0	0.05
H_{ns}	–	0	2
K_{ns}	L/g	0	0.1
k_A	1/s	10^{-10}	20
k_B	1/s	10^{-10}	20
$D_{ax,A}$	m^2/s	10^{-10}	10^{-5}
$D_{ax,B}$	m^2/s	10^{-10}	10^{-5}
a	g/L/mAU	0	0.01
b	g/L	−0.05	0.05
c	1/mAU	−0.01	0

Another drawback of GA is its inefficiency in pinpointing the final solution. GA is of stochastic nature, and works with a population of candidate solutions. In contrast, classical gradient-based methods such as SQP utilize deterministic computations (Lawrence and Tits 2001). The goal is to pinpoint the final solution with a better accuracy. Therefore, we feed the final solution obtained from GA to SQP as an initial guess. The time and computational efforts taken by the latter step is insignificant compared to the former one, but it has the advantage of a precise search around the final GA solution without the risk of falling into a local minimum. We have used this approach for both combined and separate determination of calibration and isotherm parameters.

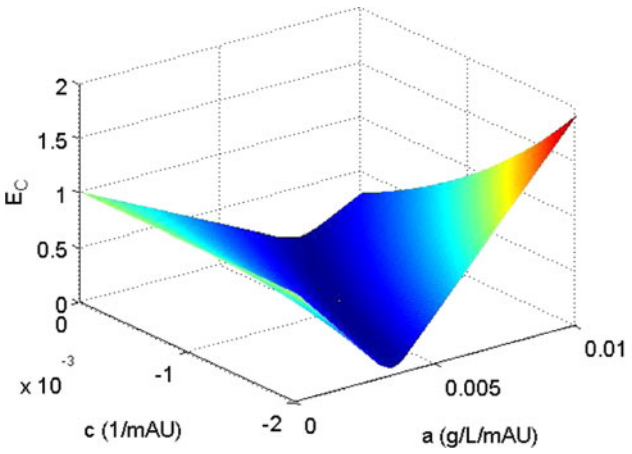

Fig. 1 Response curve of E_C for changes in the calibration parameters a and c around the optimal point obtained from NDIM using exponential calibration ($b = 4.60 \times 10^{-5}$ g/L, see Table 5)

Table 2 Simulation parameters and weight factors

Parameter	Value
ODE solver	ode113 (Shampine and Gordon 1975)
Absolute integration tolerance	10^{-6}
Relative integration tolerance	10^{-4}
Number of grid points	400
Weight factor λ_C	0.1
Weight factor λ_{I1}	0.3
Weight factor λ_{I2}	0.1

The model equations comprise partial differential equations (PDEs), which are discretized in space using third-order weighted essentially non-oscillatory (WENO) scheme (Cruz et al. 2005). This class of finite-volume based schemes is competitive to van Leer flux limiter, which was investigated in our previous work (Medi and Amanullah 2011), especially when facing large axial dispersion. The resulting set of ordinary differential equations (ODEs) is solved by the method of lines. Among different ODE solvers that we have tested, Adams-Bashforth-Moulton PECE solver (ode113) (Shampine and Gordon 1975) seemed to be the most satisfactory in terms of handling computationally intensive problems. The simulation parameters are given in Table 2. The number of grid points is chosen in such a way that numerical diffusion becomes negligible compared to axial dispersion. The weight factors introduced in Eqs. 19 and 21 are also given in Table 2.

The discretized equations were compiled in C programming language, but embedded in MATLAB environment. Parallel computing facilities of MATLAB were also utilized. In this way, the computational speed could be boosted drastically. Moreover, material balance and peak area integrations were carried out using trapezoidal rule.

4 Experimental

In this work, guaifenesin has been taken as the model chiral compound to be separated, where (S)-(+)-guaifenesin is the more retained enantiomer denoted by A and (R)-(−)-guaifenesin is the less retained enantiomer denoted by B throughout this paper. The racemic mixture of guaifenesin has been purchased from Fludan (Vankleek Hill, Canada). Heptane and ethanol solvents were used as mobile phase. The composition of the mobile phase (heptane-ethanol) for both preparative work and analysis was 65:35 (v/v). Chiralcel OD (Daicel chemical industries, Tokyo, Japan), cellulose based chiral stationary phase (cellulose tris (3,5-dimethylphenylcarbamate) coated on silica) has been considered as the preparative column (10 × 1 cm I.D., particle size 20 μm).

The overall bed void fraction (ε) was calculated using 1,3,5-tri-tert-butylbenzene (Sigma-Aldrich, Singapore) as tracer. The extra-column dead volume was also measured using the tracer injection experiments with and without the chromatographic column. Experimentally the solubility of guaifenesin in heptane-ethanol (65:35,v/v) mixture in room temperature (23 °C) has been checked and it was found near 35 g/L, which is within the range of values reported by other investigators (Francotte et al. 1998).

All raw data for isotherm determination was collected using certain parts of an existing improved single-column chromatographic (ISCC) separation process in our lab (Kazi et al. 2012). A Flexar isocratic LC pump, a six port valve, and injection loop arrangement were used for feed injection. A similar binary pump was used for pumping the mobile phase. The HPLC modules, that is, pumps, UV detectors, column oven, and degassers were purchased from PerkinElmer (Singapore). The switching valves were obtained from VICI (Schenkon, Switzerland).

Attention must be given to the proper selection of injection loop; it must have small internal diameter to suppress axial dispersion as also noted by Felinger et al. (2003). Of course the pressure drop will be higher and this may limit the minimum tubing size that can be practically used. In this work we used the largest available piece of tubing with 1/30 in internal diameter to minimize dispersion. The loop volume was obtained by measuring the mass of injection loop when filled with pure heptane and comparing it with the mass of empty loop at room temperature. These provided close match between experimental and simulated concentration profiles.

Time delay (t_d) caused by extra-column dead volume was measured and accounted for in all the reported data. Five different concentrations (10, 13, 15, 18 and 20 g/L) of guaifenesin mixture were used for the determination of isotherm parameters. In-house customized data-logging and control software developed in our laboratory were used for preparative work. The software was developed using LabVIEW (National Instruments, Singapore). The experimental conditions are summarized in Table 3.

Table 3 Experimental operating conditions

Parameter	Unit	Value
D	cm	1
L	cm	10
ε	–	0.717
d_p	μm	20
V_{inj}	μL	1192
Q_D	mL/min	2.0
t_d	s	29.0
λ	nm	295

5 Results and discussion

Results of simultaneous determination of detector calibration and isotherm parameters using NDIM are presented and compared with the classical inverse method (CIM) here. Nonlinear equations given by Eqs. 11 and 12 as well as the ubiquitous linear equation given by Eq. 10 have been used for calibration. The performance is evaluated in terms of material balance error and sum of residuals as given by the first term on the RHS of Eqs. 19 and Eq. 20, respectively. Chromatograms of all five injections have been used together for parameter estimation.

5.1 Sensitivity analysis

A sensitivity analysis can identify the importance of decision variables at least around critical points in the solution space. It can also help to locally validate optimal points. The results of a sensitivity analysis around the optimal operating point which was obtained by NDIM and exponential calibration are given in Table 4 for ±10 % change in every decision variable. The procedure is as follows: in each run only one decision variable is changed and the others remain constant at their respective optimal value. This is a straightforward method though it does not take into account interactions of decisions variables. The change in the objective function is evaluated as reported in the rows of Table 4. The results imply that all decision variables contribute to the variations of the objective function E_{I2} though at different extents. We must emphasize that the higher the sensitivity is, the higher is the reliability of the value obtained for each decision variable.

Table 4 Sensitivity analysis: change in the objective function E_{I2} for ±10 % change in the decision variables one at a time. Values are in percent with respect to the base case value of $E_{I2} = 0.0136$ and the values of decision variables given in Table 5 for exponential calibration using NDIM

	+10 %	−10 %
H_A	85.4	75.7
K_A	0.19	2.1
H_B	3.9	2.9
K_B	0.18	0.48
H_{ns}	66.1	65.3
K_{ns}	4.6	2.6
k_A	0.08	0.33
k_B	0.36	−0.15
$D_{ax,A}$	0.37	0.14
$D_{ax,B}$	−0.11	0.61
a	179.5	193.3
b	0.07	0.07
c	42.6	50.4

This method of sensitivity analysis clarifies the role of individual decision variables independently. In particular, as equilibrium constants K_A, K_B, and K_{ns} have more or less important effects on the objective function, we ensure that the experiments are overloaded enough to capture the nonlinear curvature of the bi-Langmuir isotherm up to the maximum concentration seen in the elution profiles.

5.2 Parameter estimation

The results of parameter estimation are given in Table 5. The results obtained through NDIM and CIM are almost

Table 5 Results of parameter estimation using the proposed approach (NDIM) and the classical inverse method (CIM) for various calibration equations

		CIM			NDIM		
Parameter	Unit	Rat.	Exp.	Lin.	Rat.	Exp.	Lin.
H_A	–	2.89	2.91	2.99	2.87	2.91	2.99
K_A	L/g	0.0188	0.0187	0.0221	0.0188	0.0193	0.0221
H_B	–	0.26	0.26	0.32	0.26	0.26	0.32
K_B	L/g	0.0307	0.0352	0.0483	0.0307	0.0352	0.0483
H_{ns}	–	1.21	1.17	1.16	1.21	1.17	1.16
K_{ns}	L/g	0.0414	0.0358	0.0404	0.0402	0.0350	0.0404
k_A	1/s	1.81	1.78	3.60	1.81	1.78	3.59
k_B	1/s	2.39	2.04	3.37	2.45	2.04	3.37
$D_{ax,A} \times 10^8$	m^2/s	5.07	5.43	7.69	5.07	5.50	7.72
$D_{ax,B} \times 10^8$	m^2/s	4.62	4.80	13.35	4.66	4.86	13.35
$a \times 10^3$	g/L/mAU	5.46	5.20	7.84	5.46	5.20	7.84
$b \times 10^5$	g/L	5.22	4.58	6.92	5.30	4.60	6.89
$c \times 10^3$	1/mAU	−0.405	−1.02	–	−0.405	−1.02	–

Table 6 Individual material balance and sum of residuals. The material balance errors were calculated by the first term on RHS of Eq. 19, and the sum of residuals were calculated by Eq. 20 (values are in percent)

	Material balance (%)					Sum of residuals (%)				
Sample conc. (g/L)	10	13	15	18	20	10	13	15	18	20
CIM										
Rational	−0.5	2.6	0.004	3.9	−5.0	0.6	0.6	0.6	0.8	1.0
Exponential	−0.01	2.7	−0.005	3.9	−4.8	0.5	0.5	0.5	0.7	1.0
Linear	−11.2	−1.5	0.006	7.4	3.5	0.9	0.6	0.6	0.8	0.9
NDIM										
Rational	−0.5	2.6	0.004	3.9	−5.0	0.7	0.6	0.6	0.8	1.0
Exponential	−0.01	2.7	−0.005	3.9	−4.8	0.5	0.5	0.5	0.7	0.9
Linear	−11.2	−1.5	0.006	7.4	3.5	0.9	0.6	0.6	0.8	0.9

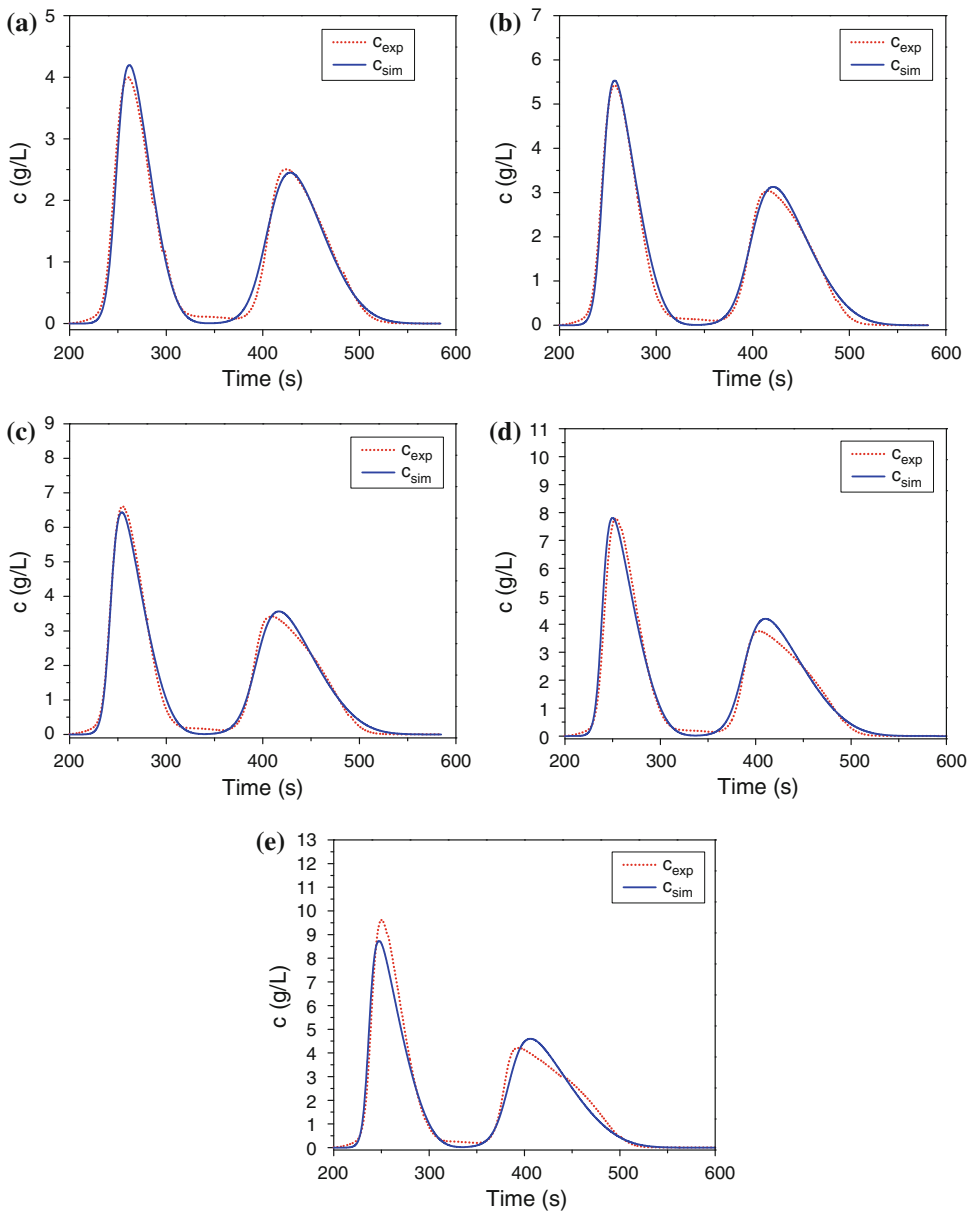

Fig. 2 Comparison of experimental and simulated elution profiles obtained by NDIM: bi-Langmuir isotherm, exponential calibration; Feed concentrations: **a** 10 g/L, **b** 13 g/L, **c** 15 g/L, **d** 18 g/L, **e** 20 g/L

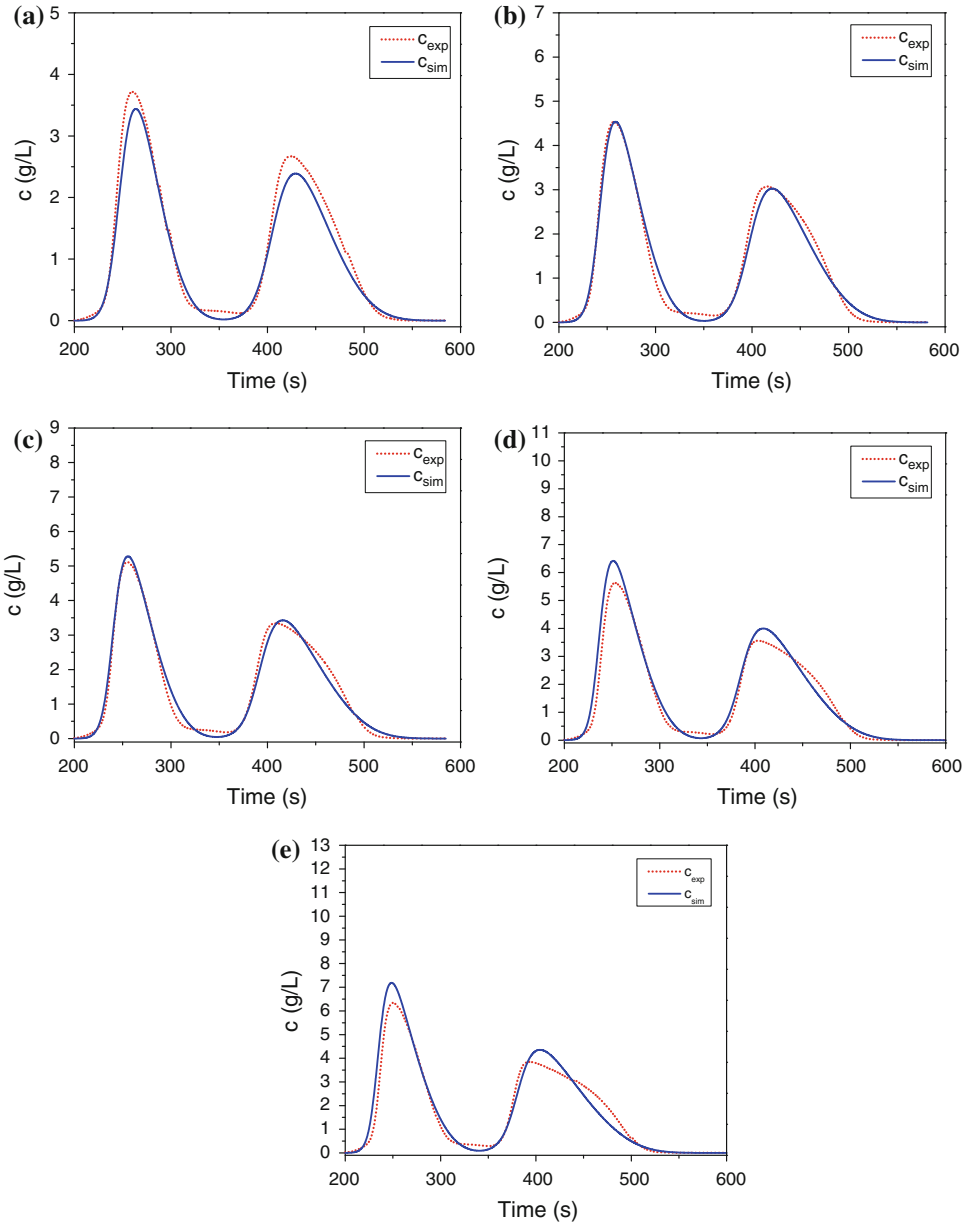

Fig. 3 Comparison of experimental and simulated elution profiles obtained by NDIM: bi-Langmuir isotherm, linear calibration; Feed concentrations: **a** 10 g/L, **b** 13 g/L, **c** 15 g/L, **d** 18 g/L, **e** 20 g/L

identical. Besides, the material balance and sum of residuals of these methods are also very similar showing that NDIM approach is as good as the classical one (see Table 6) while the former allows simultaneous determination of calibration and isotherm parameters.

Looking at Table 5, the values of non-selective parameters of bi-Langmuir isotherm are comparable to selective ones indicating that there are at least two types of sites available for adsorption. Therefore, simpler isotherms such as ordinary Langmuir are inadequate for describing the separation behavior though the cumulative Henry constants (i.e., $H_i + H_{ns}$) obtained here are close to what reported by Francotte et al. (1998) using a Langmuir isotherm. On the other hand, this observed amount of non-selective adsorption suggests a better experimental operating condition must be sought for preparative work.

The estimated axial dispersion coefficients are in the range of correlations given by Butt (1980) and Guiochon et al. (2006). However, the mass transfer coefficients are smaller than what reported by Zabka et al. (2008) and Phillips et al. (1988). This could be due to the distortion in the boundary condition caused by imperfect injection mechanism.

The comparison of experimental and simulated elution profiles using NDIM is shown in Figs. 2 and 3 for exponential and linear calibrations, respectively. It is clear from these figures that the matches are much better for experimental calibration compared to the linear one. The results

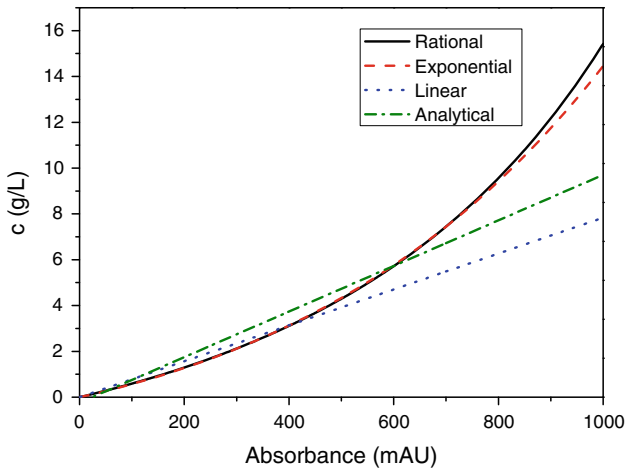

Fig. 4 Calibration curves obtained using NDIM as given in Table 5. The line obtained by the analytical method (Eqs. 17 and 18) is also given for comparison. Note that the calibration equations are just valid up to the maximum concentration observed on the elution profiles (ca 10 g/L)

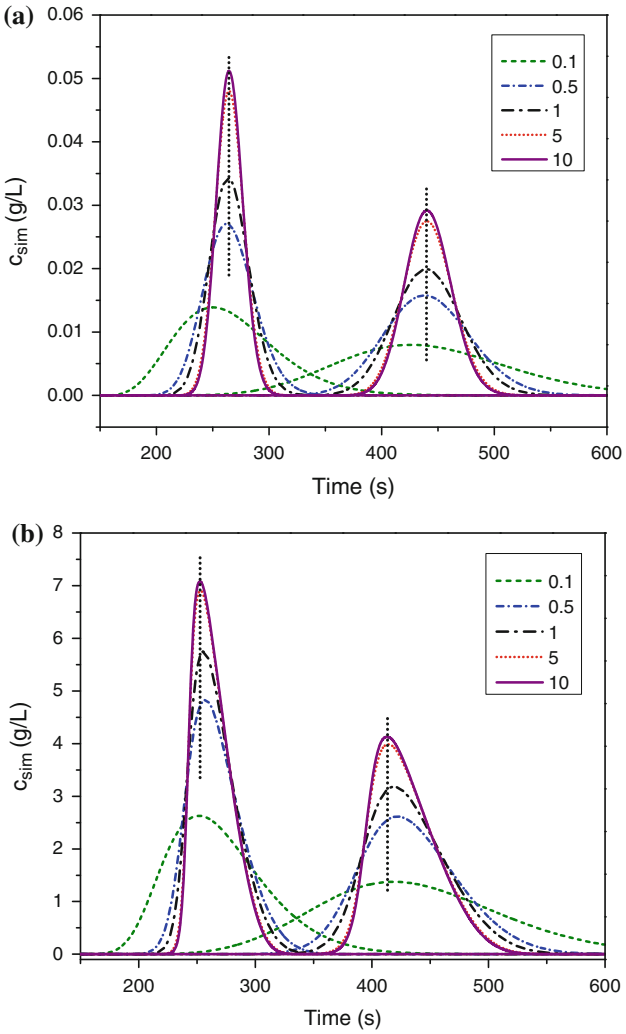

Fig. 5 Effects of change in mass transfer coefficients; **a** analytical injections ($V_{inj} = 100$ µL, $c_T^F = 1$ g/L **b** overloaded injections ($V_{inj} = 1192$ µL, $c_T^F = 15$ g/L.). The legends are mass transfer coefficients for both components in 1/s. The *vertical lines* designate the peak position for $k_i = 10$ 1/s. The simulated chromatograms were produced near optimal points obtained using NDIM

also show that nonlinear calibration with bi-Langmuir isotherm satisfactorily describes the separation behavior of guaifenesin enantiomers on Chiralcel OD stationary phase using heptane-ethanol (65:35, v/v) mobile phase. Results of the rational calibration are very similar to the exponential one.

The material balance and sum of residuals obtained using CIM and NDIM methods are given in Table 6. The material balance error is less than 5 % for the rational and exponential calibrations, which is acceptable for this type of separation problem, but it is large for linear calibration indicating inadequacy of the linear calibration.

It is very important to note that the sums of residuals are all small and acceptable (see Table 6). However, these results can be misleading if the material balance error is not accounted for at the same time. Table 5 shows that rational and exponential calibration equations have resulted in similar estimated parameters, but the results obtained through linear calibration are significantly different. This difference is mainly manifested in the material balance error though calibration parameters slightly affect sum of residuals as well (see Table 6). This finding suggests that an inaccurate calibration may bring about results that offer good fit to the experimental elution profiles, but will seriously violate the material balance. Therefore, in any parameter estimation problem, the material balance error, which is primarily regulated by the calibration equation, must be included as a part of the objective function. Of course the minor effect of calibration parameters on sum of residuals can also be better exploited in NDIM and may facilitate the convergence. These are in fact major advantages of the proposed method, which simultaneously takes into account material balance and sum of residuals.

5.3 Calibration curves

The calibration curves are plotted in Fig. 4 using the estimated parameters obtained by NDIM given in Table 5. For comparison, we have also added the line obtained by analytical calibration, i.e. calculating the peak areas and using Eqs. 17 and 18. For detector calibration, this method gives inferior fit and seriously violates the material balance. Both of the nonlinear calibration equations, i.e. rational and exponential, provide similar results. In fact, they are practically identical at lower absorbance values and differ slightly at higher values as seen in the figure. On

the other hand, it is clear that the method presented for linear calibration in this paper is more accurate than the analytical approach.

5.4 Effects of transport parameters

To investigate the distinct contributions of mass transfer and dispersion effects, simulations have been carried out by changing mass transfer coefficients, k_i, both at low and overloaded conditions near optimal points obtained using NDIM as shown in Fig. 5. It is clear from the figure that, as expected, band broadening is a function of mass transfer coefficient, but retention time is not affected by this parameter in the linear range of operation, except for very small k_i values. On the other hand, in the overloaded range of operation, the peak position is clearly shifted with varying k_i values. This asymmetric change cannot be explained by axial dispersion as its effect is merely symmetrical in usual operating conditions (except under very large dispersion, (Levenspiel 1999). Therefore, a mathematical model that accounts for mass transfer resistance separately (i.e., differentiating it from axial dispersion), is more appropriate when dealing with complex isotherms such as bi-Langmuir.

6 Concluding remarks

For majority of dynamic methods, detector calibration is a prerequisite step to isotherm determination though there are a few exceptions (e.g., PM). We have presented a method for simultaneous calibration of detector and determination of adsorption isotherm. It can readily be used for a mixture of enantiomers under base line separation or overlapping of elution profiles. For achiral compounds however, the chromatogram must be baseline separated to be processed by this method. This method is faster and more economical than other alternatives provided that efficient computational facilities are available.

We have shown that this method can reduce the risk of converging to a wrong calibration equation that violates material balance and subsequently a wrong set of isotherm parameters. This is achieved through simultaneous calibration and isotherm determination in a single step. This is indeed an advantage of our approach compared to the CIM.

We have used a hybrid optimization method for parameter estimation as this problem suffers from several local minima. GA in conjunction with SQP algorithm have been used to globally search for the optimum set of parameters and pinpoint the final solution, respectively. Faster convergence was achieved through improved formulation of the objective function.

We also proposed alternative nonlinear calibration equations. This is a major difference compared to the DIM, which is limited to linear calibration because of its solution approach. Preparative chromatography necessitates nonlinear calibration to ensure detector sensitivity over a wide range of feed concentration and this method is expected to be useful for determination of calibration and isotherm parameters in a single step.

It appears that there is a gap in research regarding detector calibration under overloaded chromatographic conditions for generic compounds, not just enantiomers, which can be a useful subject of future work in this area.

Acknowledgments The authors thank Singapore's Ministry of Education for supporting this work through Grant No. RG24/07.

References

Amanullah, M., Mazzotti, M.: Optimization of a hybrid chromatography-crystallization process for the separation of troger's base enantiomers. J. Chromatogr. A **1107**(1–2), 36–45 (2006)

Asnin, L., Guiochon, G.: Calibration of detector responses using the shape and size of band profiles: case of a nonlinear response curve. J. Chromatogr. A **1089**(1–2), 101–104 (2005)

Asnin, L., Galinada, W., Gotmar, G., Guiochon, G.: Calibration of a detector for nonlinear chromatography. J. Chromatogr. A **1076**(1–2), 141–147 (2005)

Blumel, C., Hugo, P., Seidel-Morgenstern, A.: Quantification of single solute and competitive adsorption isotherms using a closed-loop perturbation method. J. Chromatogr. A **865**(1–2), 51–71 (1999)

Butt, J.B.: Reaction Kinetics and Reactor Design. Prentice Hall, Englewood Cliffs (1980)

Cornel, J., Mazzotti, M.: Calibration-free quantitative application of in situ raman spectroscopy to a crystallization process. Anal. Chem. **80**(23), 9240–9249 (2008)

Cornel, J., Tarafder, A., Katsuo, S., Mazzotti, M.: The direct inverse method: a novel approach to estimate adsorption isotherm parameters. J. Chromatogr. A **1217**(12), 1934–1941 (2010)

Cruz, P., Santos, J.C., Magalhpes, F.D., Mendes, A.: Simulation of separation processes using finite volume method. Comput. Chem. Eng. **30**(1), 83–98 (2005)

Dunnebier, G., Klatt, K.U.: Modelling and simulation of nonlinear chromatographic separation processes: a comparison of different modelling approaches. Chem. Eng. Sci. **55**(2), 373–380 (2000)

Felinger, A., Cavazzini, A., Guiochon, G.: Numerical determination of the competitive isotherm of enantiomers. J. Chromatogr. A **986**(2), 207–225 (2003)

Francotte, E., Richert, P., Mazzotti, M., Morbidelli, M.: Simulated moving bed chromatographic resolution of a chiral antitussive. J. Chromatogr. A **796**(2), 239–248 (1998)

Goldberg, D.E.: Genetic Algorithms in Search, Optimization and Machine Learning. Addison-Wesley, New York (1989)

Golshanshirazi, S., Guiochon, G.: Comparison of the various kinetic-models of nonlinear chromatography. J. Chromatogr. **603**(1–2), 1–11 (1992)

Guiochon, G.: Preparative liquid chromatography. J. Chromatogr. A **965**(1–2), 129–161 (2002)

Guiochon, G., Fellinger, A., Shirazi, D.G., Katti, A.M.: Fundamentals of Preparative and Nonlinear Chromatography, 2nd edn. Academic Press, Boston (2006)

Juza, M., Mazzotti, M., Morbidelli, M.: Simulated moving-bed chromatography and its application to chirotechnology. Trends Biotechnol. **18**(3), 108–118 (2000)

Kazi, M.K., Medi, B., Amanullah, M.: Optimization of an improved single-column chromatographic process for the separation of enantiomers. J. Chromatogr. A **1231**, 22–30 (2012)

Lawrence, C.T., Tits, A.L.: A computationally efficient feasible sequential quadratic programming algorithm. Siam. J. Optim. **11**(4), 1092–1118 (2001)

Levenspiel, O.: Chemical Reaction Engineering, 3rd edn. Wiley, New York (1999)

Lisec, O., Hugo, P., Seidel-Morgenstern, A.: Frontal analysis method to determine competitive adsorption isotherms. J. Chromatogr. A **908**(1–2), 19–34 (2001)

Mazzotti, M.: Local equilibrium theory for the binary chromatography of species subject to a generalized langmuir isotherm. Ind. Eng. Chem. Res. **45**(15), 5332–5350 (2006)

Medi, B., Amanullah, M.: Application of a finite-volume method in the simulation of chromatographic systems: effects of flux limiters. Ind. Eng. Chem. Res. **50**(3), 1739–1748 (2011)

Phillips, M.W., Subramanian, G., Cramer, S.M.: Theoretical optimization of operating parameters in non-ideal displacement chromatography. J. Chromatogr. A **454**(C), 1–21 (1988)

Rajendran, A., Chen, W.: Binary retention time method for rapid determination of competitive langmuir isotherm parameters. Sep. Purif. Technol. **67**(3), 344–354 (2009)

Ruthven, D.M.: Principles of Adsorption and Adsorption Processes. Wiley, New York (1984)

Seidel-Morgenstern, A.: Experimental determination of single solute and competitive adsorption isotherms. J. Chromatogr. A **1037**(1–2), 255–272 (2004)

Shampine, L.F., Gordon, M.K.: Computer Solution of Ordinary Differential Equations: The Initial Value Problem. W. H. Freeman and Co., San Francisco (1975)

Soussen-Jacob, J., Tsakiris, J., De Lara, E.C.: Adsorption of oxygen molecule in NaA zeolite: isotherms and infrared measurements. J. Chem. Phys. **91**(4), 2649–2655 (1989)

Thompson, K.A., Fuller, J.E.L.: Accurate sorption isotherms using a computer-aided microgravimetric method. J. Vac. Sci. Technol. A **5**(4), 2522–2525 (1987)

Wenda, C., Rajendran, A.: Enantioseparation of flurbiprofen on amylose-derived chiral stationary phase by supercritical fluid chromatography. J. Chromatogr. A **1216**(50), 8750–8758 (2009)

Zabka, M., Minceva, M., Gomes, P.S., Rodrigues, A.E.: Chiral separation of R,S-α-tetralol by simulated moving bed. Sep. Sci. Technol. **43**(4), 727–765 (2008)